JOURNAL OF ENERGY, MATERIALS, AND INSTRUMENTATION TECHNOLOGY

Journal Webpage https://jemit.fmipa.unila.ac.id/

FTIR, XRD, and SEM-EDX Characterization of Synthesized B-Type Carbonated Hydroxyapatite (CHAp) Based on Crab Shells

Muhamad Fajar Muarif[1*], Yusril Yusuf[2], and Ade Irmadiki Agipa[3]

1. Study program of physics, Universitas Islam Negeri Sultan Maulana Hasanuddin, Banten, Indonesia, 42118
2. Departement of Physics, Universitas Gadjah Mada, Yogyakarta, Indonesia, 55281
3. Study program of chemistry, Universitas Islam Negeri Sultan Maulana Hasanuddin, Banten, Indonesia, 42118

Article Information

Article history:
Received January 22, 2024
Received in revised form January 24, 2024
Accepted January 25, 2024

Keywords: *B-Type CHAp, FTIR, XRD, SEM-EDX, Crab Shells*

Abstract

The synthesis and characterization of B-type CHAp based on mangrove crab shells (Scylla serrata) as a source of calcium using the precipitation method has been successfully carried out. Based on the FTIR results, the substitution of carbonate ion for phosphate, which indicates the formation of B-type CHAp, is characterized by the appearance of absorption at wave numbers (CO_3^{2-}) 1426 and *875 cm^{-1}, PO_4^{3-} at wave numbers 965, 619 & 569 cm^{-1}. The XRD results show that diffraction peaks (211), (300), and (202) appear at an angle of 2θ ranging from 31°-34°, and there is a phenomenon of a-axis contraction and c-axis expansion in the HAp lattice structure. The SEM-EDX results show that the Ca/P ratio is 1.72, and the carbonate content is 5.01 wt%. All of these parameters are characteristics of CHAp, so it can be concluded that type-B CHAp has been formed.*

Informasi Artikel

Proses artikel:
Diterima 22 Januari 2024
Diterima dan direvisi dari 24 Jnauari 2024
Accepted 25 Januari 2024

Kata kunci: *CHAp Tipe B, FTIR, XRD, SEM-EDX, Cangkang Kepiting,*

Abstrak

Sintesis dan karakterisasi CHAp tipe B berbahan dasar cangkang kepiting bakau (Scylla serrata) sebagai sumber kalsium menggunakan metode presipitasi telah berhasil dilakukan. Berdasarkan hasil FTIR, substitusi ion karbonat pada fosfat yang mengindikasikan terbentuknya CHAp tipe B ditandai dengan munculnya serapan pada bilangan gelombang (CO_3^{2-}) 1426 and 875 cm^{-1}, PO_4^{3-} pada bilangan gelombang 965, 619 & 569 cm^{-1}. Hasil XRD menunjukkan mucul puncak difraksi (211), (300), dan (202) pada sudut 2θ berkisar 31°-34°, dan terjadi Adanya fenomena kontraksi sumbu a dan ekspansi sumbu c pada struktur kisi HAp. Hasil SEM-EDX menjelaskan bahwa rasio Ca/P adalah 1,72 dan kandungan karbonat sebesar 5.01 wt%. Semua parameter tersebut merupakan karakteristik dari CHAp sehingga dapat disimpulkan bahwa telah terbentuk CHAp tipe B.

1. Introduction

Indonesia is rich in natural resources, one of which comes from aquaculture, such as shrimp, lobster, tuna, seaweed, crab, etc. Crab is one of the most popular foods in the world. Based on data from Environmental Statistics, crab is the main export commodity, with a capacity of 27,616 tons in 2020 (Badan Pusat Statistik, 2021). High consumption of crabs causes problems with waste coming from their shells. Ratri (2021) examined the content of the crab shell, which is around 75% of the total weight of the crab. Abandoned crab shell waste will cause environmental problems aesthetically and in ecosystem stability.

Crab shells contain CaO compounds of 71.42%, MgO of 4.81%, P_2O_5 of 3.98%, C of 19.78%, and O of 24.53% (Haryati et al., 2019). The high calcium content in crab shells can be used as a biomaterial, especially in forming apatite compounds. One of the uses of biomaterials from apatite compounds is bone implants because they have a chemical composition similar to bone minerals. Biomaterials that are applied in the body must meet criteria such as biocompatible so that resistance reactions do not occur in the body, non-toxic and non-inflammatory so that

* Corresponding author.
E-mail address: muhamad.fajar@uinbanten.ac.id

they are not harmful to the body, bioactive so they can be digested by bone cells, biodegradable and bioresorbable so that they can be decomposed and can be absorbed by cells osteoclasts in bones, and resemble the constituent components of the body whose composition is similar to the bones in the body. The apatite group compound widely used in bone implants is Hydroxyapatite (HAp).

Hydroxyapatite (HAp) with the chemical formula $Ca_{10}(PO_4)_6(OH)_2$ is a bioceramic from the calcium phosphate (CaP) crystal family, which is widely used as a bone implant material due to its similar composition (Ratner et al., 2013). As a bone implant material, Hap also has weaknesses; HAp's stoichiometry does not dissolve over time, so the rate of bio-resorptive replacement of new bone that grows becomes slow (Bang et al., 2014)(Filippov et al., 2011). Substituting carbonate ions on Hap is known to increase the solubility or absorption of HAp (E Landi et al., 2003).

Carbonate hydroxyapatite (CHAp) is HAp substituted by carbonate ions (Surbakti et al., 2017). CHAp, with a carbonate composition ranging from 2-8%, is known to be more similar to bone structure compared to HAp compounds. Carbonate ion (CO_3^{2-}) can be substituted at three different locations of the HAp lattice structure. A-Type CHAp is formed when carbonate ions displace hydroxide groups and are found in old bone tissue. B-type CHAp is created when a carbonate ion replaces a phosphate group, whereas AB-type CHAp occurs when a carbonate ion replaces a phosphate and hydroxide group (Gibson & Bonfield, 2001). In general, B-type CHAp is preferred because it is found in many young tissues due to its high solubility or absorption, both in vitro and in vivo (Barralet et al., 2000)(Landi et al., 2004)

In this research, B-type CHAp material was synthesized using the precipitation method. This method is one of the most widespread approaches because it is simple, uses relatively cheap raw materials, and can be combined with low temperatures to lower operational costs (Yusuf et al., 2021). The success parameters of the synthesis of B-type CHAp can be seen based on the Ca/P mole ratio >1.67, c/a value >0.7309, low crystallinity, small crystallite, and particle sizes, and the weight percentage of carbonate ranging from 2-8 wt.% (Safarzadeh et al., 2019). Sintering temperatures were used to determine the crystallographic properties of CHAp, such as phase crystallinity, grain size, and surface topography (Germaini et al., 2017). Chemical characterization using FTIR spectrophotometer to see the CHAp functional groups and X-ray diffractometer (XRD) to see the crystalline phases formed, while physical characterization using X-ray diffractometer (XRD) to see crystallinity, surface morphology using an electron microscope (SEM).

2. Research Methods

2.1 Materials

Materials for CHAp synthesis use calcium oxide (CaO) from mangrove crab shells *(Scylla serrata)* as a source of natural calcium (Ca). Ammonium bicarbonate (NH_4HCO_3) (Merck, Germany) as a source of carbonate (CO_3^{2-}). Diammonium hydrogen phosphate $(NH_4)_2HPO_4$ as a source of phosphate (P) (Merck, Germany). During the synthesis process, the pH controller uses ammonium hydroxide (NH_4OH) (Merck, Germany) to keep the pH of the solution at pH ≥ 10. Distilled water (H_2O) is a solvent in the synthesis process. Acetone liquid (C_3H_6O) is used to help the drying process of laboratory equipment.

2.2 CaO Preparation

Crab shells were collected and washed using distilled water to remove impurities on the shell. Then, the crab shells were boiled in distilled water to remove impurities and organic residues for 30 minutes and soaked in acetone in a closed container for three days with the replacement acetone every 1x24 h. After three days, it was dried in the oven at 100°C for 4 hours to assist in drying the water content in the shells. Dried samples are powdered by crushing them using a ball mill to get calcium carbonate ($CaCO_3$) powder. It calcinates using a furnace at 1000°C for 4 h to obtain CaO powder.

2.3 CHAp Synthesis

The CHAp was synthesized from crab shells by mixing a CaO source derived from crab shells, a phosphate source from $(NH_4)_2HPO_4$, and a carbonate source from NH_4HCO_3. In the initial step, the CaO powder was sieved using a 170 mesh and 6,16 grams of filtered CaO powder dissolved in 80 ml of distilled water to make 0.11 mol CaO solution with stirring for one hour at 350 rpm. $(NH_4)_2HPO_4$ 8,712 grams was dissolved in 80 ml of distilled water and stirred at 350 rpm at room temperature to make a solution of $(NH_4)_2HPO_4$ 0,066 mol. The pH was controlled by adding 18 ml of NH_4OH while still stirring until the solution was formed alkaline or reached a pH ≥ 10. They dissolved 5,214 grams of NH_4HCO_3 in 50 ml of distilled water as a carbonate source while stirred at 350 rpm at room temperature to make 0,066 mol of NH_4HCO_3. Mixing the NH_4HCO_3 solution into the $(NH_4)_2HPO_4$ solution was added dropwise at a rate of 1 ml/min at room temperature and stirring for 10 minutes at 350 rpm.

In the last step, mixing $(NH_4)_2HPO_4$ + NH_4HCO_3 into the $Ca(OH)_2$ solution was added dropwise at 1 ml/min and stirred at 350 rpm at 2 h. The solution was precipitated for 24 hours at room temperature until a precipitate formed on the bottom of the beaker glass. The precipitate was filtered using Whatman 41 filter paper with a diameter of 90 mm overnight and centrifuged 3 times (4800 rpm, 10 minutes) to remove another ion. The resulting precipitate was dried at 70°C overnight, crushed, and filtered using a 170 mesh sieve to produce a relatively homogeneous grain size. The sieve results were heated at 700°C for 2 h in a furnace.

2.4 Characterization

Sample characterization was carried out in two stages. The first stage characterizes the results of the sample preparation. At this stage, the sample characterization uses FTIR, SEM-EDX, and XRD to determine the group

function, calcium (Ca) content, and morphology, as well as the crystallographic properties of the sample. The second step is the characterization of the synthesis results. The characterization at this stage used FTIR to determine the functional groups of OH-, PO_4^{3-}, and CO_3^{2-} in the sample, SEM-EDX to determine the proportion by weight of carbonate in the CHAp structure (2-8wt%), and the morphology of the synthesized CHAp powder. XRD was used to determine the crystal structure of the CHAp sample.

3. Results and Discussions

3.1 Calcium carbonate ($CaCO_3$)

Initial testing in this study was carried out to confirm the presence of $CaCO_3$ in crab shells. XRD tests produced the resulting diffraction pattern in **Figure 1 (a)**. The diffraction results show agreement with the $CaCO_3$ diffraction peaks and are matched with commercial JCPDS $CaCO_3$ data number 085-1108 (Rujitanapanich et al., 2014). The crystal plane representing $CaCO_3$ is at an angle of 23.345°, 47.948°, 48.952° and 57,936°.

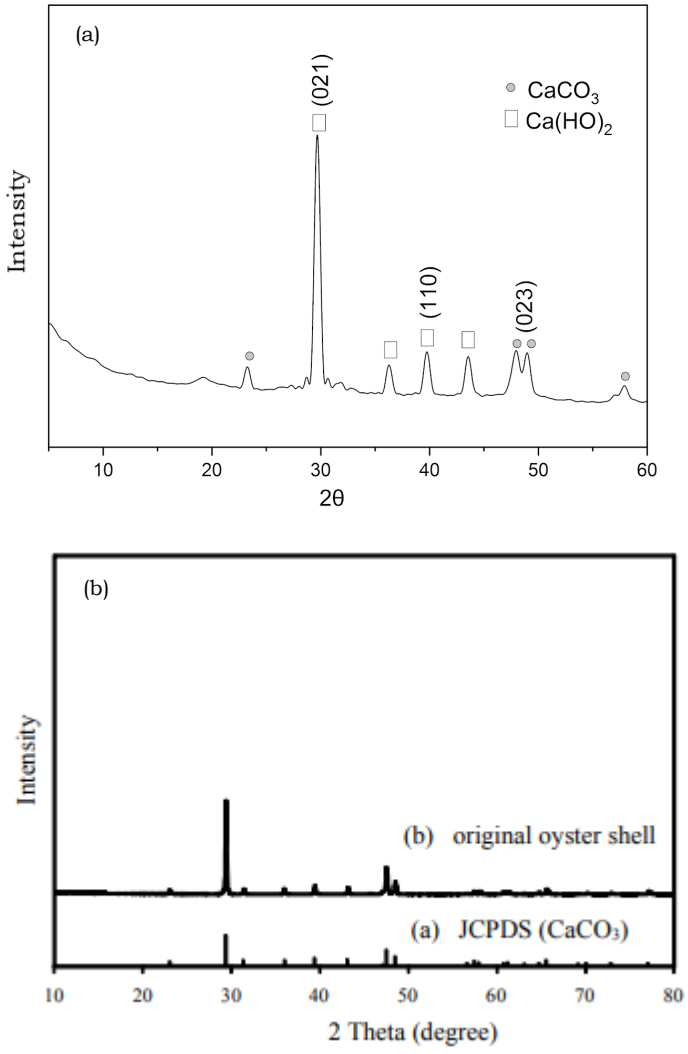

Figure 1. (a) XRD pattern of $CaCO_3$ from this research, (b) XRD pattern of $CaCO_3$ (Rujitanapanich et al., 2014)

The highest intensity of the main diffraction peak is formed at an angle of 2θ=29.683° followed by other peaks with smaller intensities such as 23.219°, 36.239°, 39.785°, 43.525°, 47.983° 48.986° and 57.902°. The XRD diffraction pattern produced from crab shells is similar to the XRD diffraction pattern created in Rujitanapanich et al.'s (2014) research, which can be seen in **Figure 1 (b)**. Some peaks correspond to the diffraction planes characteristic of $CaCO_3$, namely the (021) plane at an angle of 29.683° and the (110) plane at an angle of 39.785₀, thus strengthening that the crab shell powder is $CaCO_3$.

The EDX results confirmed the existence of several phases of impurities in the CaCO3 of crab shells. Quantitatively, the constituent elements detected from the EDX results in crab shell powder, carbon, oxygen, sodium, calcium, and copper, with weight percentages as in **Table 1**.

Table 1. Weight percentage of elements in crab shell powder

Element	Weight percentage (wt.%)
C	19.86
O	50.84
Na	0.30
Ca	26.34
Cu	2.66

Based on **Table 1**, we can find out the weight percentage of each element contained in the sample. The Ca element identified was 26.34 wt.%, which confirmed that the calcium content in the sample was quite abundant. Ca is needed in the CHAp synthesis process because it is one of the main contents of CHAp (Yusuf et al., 2021). Therefore, the sample remains the basic material for CHAp synthesis.

3.2 Calcium Oxide (CaO)

CaO identification was carried out using XRD and EDX tests. The XRD results of crab shell CaO powder were identified by comparing the diffraction peaks formed with JCPDS number 37-1479. The diffraction pattern of the XRD results of crab shell CaO is at an angle of 50,935°, as seen in **Figure 2**.

In this research, crab shell $CaCO_3$ was calcined at a temperature of 1000 °C to obtain CaO as a source of calcium in the CHAp synthesis process. The 1000 °C temperature treatment is a calcination treatment. Calcination is a heating process using high temperatures. The aim of using high temperatures is to decompose the CaCO3 content to be CaO. The high temperature breaks the chemical bonds between calcium and carbon, releasing CO_2 from $CaCO_3$ to form CaO. After the calcination process, 26.639 grams of $CaCO_3$ was reduced to CaO 12.823 with an efficiency of 51.86%. The reduction in mass after calcination is caused by the release of CO_2 compounds during the calcination process

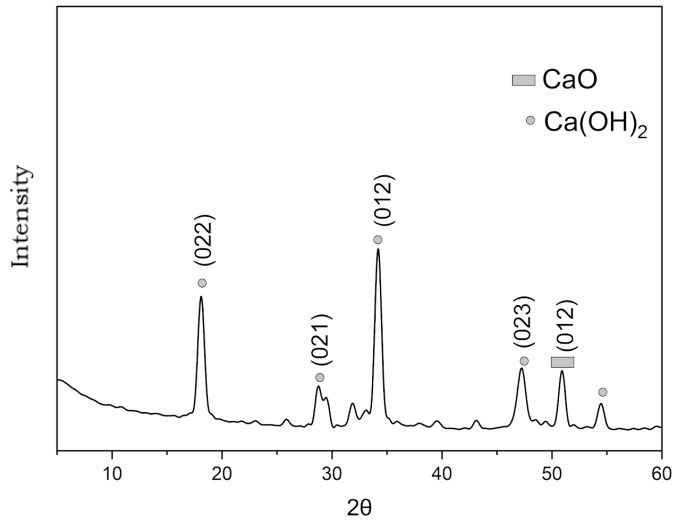

Figure 2. CaO XRD pattern of mangrove crab shell

The results of XRD analysis show a phase change from $CaCO_3$ to CaO. However, these results also show another phase formed, namely the $Ca(OH)_2$ phase. The phase change from CaO to $Ca(OH)_2$ usually occurs at high temperatures after calcination. The appearance of this phase occurs due to changes in temperature during calcination, causing vibrations of the atoms containing the nucleus in the sample to combine and form a new phase. The transformation process of CaO into $Ca(OH)_2$ is formed by the spontaneous pyrogenic reaction of $CaCO_3$, which is subjected to water content in the atmospheric air over a long period during the cooling process (Ruiz et al., 2009). The decomposition process at high temperatures causes CaO to be hydrated with a marked reduction in CaO reactivity. The hydration process that occurs can be seen in **Equation 1**.

$$CaO+H_2O \rightarrow Ca(OH)_2 \quad (1)$$

3.3 Characterization Results of Carbonate Hydroxyapatite Base on Crab Shell

3.3.1 The FTIR results

The FTIR results for CHAp are shown in **Figure 3**. The spectrum shows the characteristic bands of the PO_4^{3-} a group from the apatite structure in the doublet bands 569 and 619 cm^{-1} and 965 cm^{-1}. The substitution of carbonate ion for phosphate indicates the formation of type-B CHAp, which showed CO_3^{2-} in apatite can be detected at 1426 and 875 cm^{-1}. This result confirms the type B substitution in apatite (Wati & Yusuf, 2019). This type of substitution is preferred in biological bone and is commonly found in young tissue. The formation of type-B CHAp also causes a decrease in crystallinity and provides better solubility (Landi et al., 2004).

Muarif MF, Yusuf Y, and Agipa AI, 2024, FTIR, XRD, and SEM-EDX Characterization of Synthesized B-Type Carbonated Hydroxyapatite (CHAp) Based on Crab Shells, *Journal of Energy, Material, and Instrumentation Technology* Vol. 5 No. 1, 2024

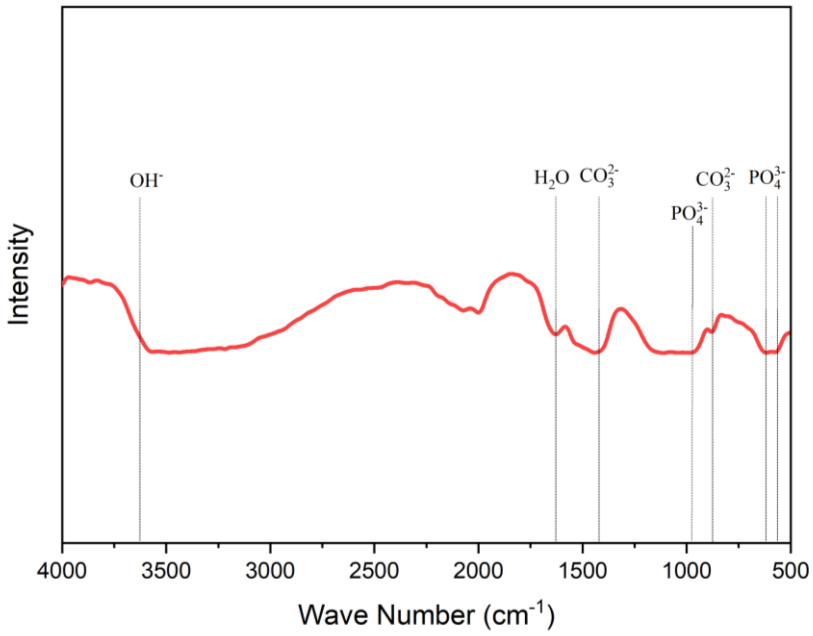

Figure 3. FTIR spectra of synthesizing B-type CHAp from crab shells.

The successful synthesis of B-type CHAp made from mangrove crab shells can be seen in Figure 3, which shows the presence of PO_4^{3-}, OH-, and CO_3^{2-} groups. Substitution of the CO_3^{2-} ion, which has characteristics of B-type carbonate absorption (CHAp B-type), is demonstrated by stretching vibrations in the wave number region 1410-1477 cm^{-1} and 875-924 cm^{-1} (Ezekiel et al., 2018). Jayasree et al. (2018) also reported the substitution of CO_3^{2-} ions for phosphate ions (PO_4^{3-}) in their research, which stated that there was group absorption in the wave number area 1410-1477cm^{-1}.

A summary of the absorption bands for the functional groups PO_4^{3-}, OH-, CO_3^{2-}, and water absorption can be seen in **Table 2**.

Table 2. Summary of FTIR CHAp spectra from crab shells

Functional groups	Wave Number (cm^{-1})
PO_4^{3-}	965, 619 & 569
CO_3^{2-}	1426 & 875
OH^-	3600
H_2O	1628

3.3.2 The XRD results

The CHAp XRD results from mangrove crab shells are explained by comparing the diffraction peaks formed with those in JCPDS No. 09-0432. The XRD pattern of the CHAp sample shows broadened diffraction peaks visible in the range 2θ≈31-34o corresponding to the (211), (300), and (202) diffraction planes. In general, all CHAp samples of crab shells have similarities with the characteristic diffraction peaks of the apatite structure, as seen in **Figure 4**.

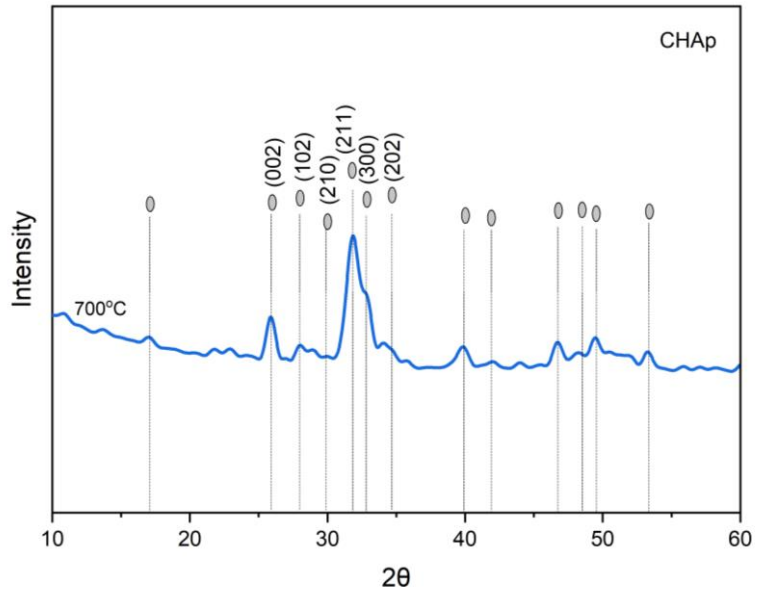

Figure 4. XRD pattern of synthesizing type-B CHAp from crab shells

The XRD results show that the main diffraction peaks are formed in the diffraction planes (211), (300), and (202). More specifically, the diffraction plane (211) corresponds to an angle of 31.838°, (300) to an angle of 32.813°, and (202) to an angle of 34.108°. JCPDS Data No. 09-0432 shows that the HAp phase has main diffraction peaks at diffraction angle positions 31.77°, 32.90°, and 34.04°. In other words, the XRD spectrum data formed is related to the position of the main diffraction peaks of the HAp phase. However, compared with the JCPDS HAp data, it can be seen that there is a shift in the position of the main diffraction angles of the synthesized sample towards larger diffraction angle values. Pieters et al. (2010) suggested that the shift in the position of the diffraction angle in the diffraction planes (211), (300), and (202) towards a larger diffraction angle value was caused by the substitution of carbonate ions in the HAp lattice structure which caused contraction of the apatite unit cell in the a-lattice structure of HAp.

Analysis of the (002) diffraction plane shows a shift in the diffraction angle from the (002) diffraction plane towards a smaller diffraction angle value. Based on JCPDS HAp data, the diffraction plane (002) is formed at a diffraction angle of 25.879°, while the resulting diffraction angle of 25.827° has an error value of 0.052°. This shift indicates the presence of carbonate ion substitution in the HAp lattice structure, which represents the expansion of the apatite unit cell along the c-axis. This substitution of carbonate ions in the HAp lattice structure confirmed that the sample had changed to the CHAp phase. The phenomenon of a-axis contraction and c-axis expansion in the HAp lattice structure is characteristic of the B-type carbonate ion substitution phenomenon, indicating B-type CHAp formation (Pieters et al., 2010).

3.3.3 The SEM-EDX results

The characterization results using SEM show a picture of the morphology of the CHAp sample from crab shells, shown in **Figure 5**. Visually, agglomeration can be seen in the morphology of the CHAp sample. Nanomaterials have a large specific surface area, so they are unstable and form an agglomeration state (Kadarisman & Nurhasanah, 2020). Agglomeration occurs because particles interact with each other (Melinia et al., 2022), thus creating larger clumps of particles. This interaction is caused by the presence of quite strong electrostatic forces on the particles (Desiati et al., 2018), apart from being influenced by humidity due to the presence of H2O on the surface of the nanoparticles. The surface looks uneven because of the presence of small, irregular particles that stick irregularly to the surface of the grain. The grain size of the sintered CHA sample can be seen in **Figure 5**.

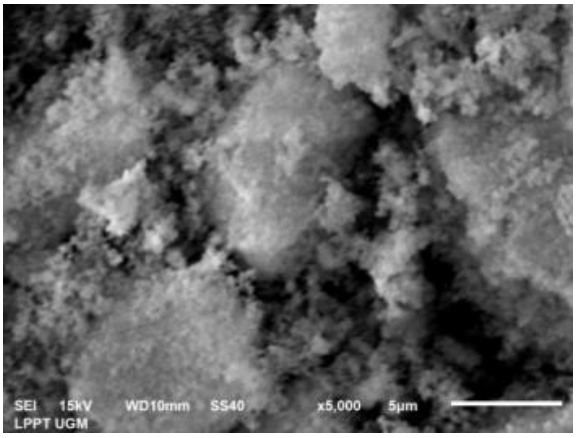

Figure 5. The morphology of the CHAp sample from crab shells

EDX results show the Ca/P ratio and carbonate content of crab shell CHAp samples. The Ca/P ratio shows 1.72; this value is greater than the Ca/P ratio in HAp (1.67), which shows that there is a substitution in the carbonate content in the sample, which is confirmed by the EDX results that there is 5.01 wt% carbonate. These results fall into the range of carbonates in natural bone, which ranges from 2-8wt% (Wong & Noor, 2016).

4. Conclusions

The synthesis and characterization of B-Type CHAp made from crab shells (*Scylla serrata*) using the precipitation method have been successfully carried out. The sample characterization uses FTIR, SEM-EDX, and XRD. Based on the FTIR results, CO32- absorption appears at wave numbers 1426 and 875 cm^{-1} and PO_4^{3-} at wave numbers 965, 619, and 569 cm^{-1}. The XRD results show that diffraction peaks (211), (300), and (202) appear at an angle of 2θ=31°-34° and a phenomenon of a-axis contraction and c-axis expansion in the HAp lattice structure. The SEM-EDX results are that the Ca/P ratio is 1.72, and the carbonate content is 5.01 wt% into the range of carbonates in natural bone (2-8 wt%). All of these parameters are characteristics of CHAp, so it can be concluded that B-type CHAp has been formed.

5. Bibliography

Badan Pusat Statistik. (2021). *Statistik Lingkungan Hidup Indonesia 2021 Energi dan Lingkungan* (Subdirektorat Statistik Lingkungan Hidup (ed.)). Badan Pusat Statistik.

Bang, L. T., Long, B. D., & Othman, R. (2014). Carbonate Hydroxyapatite and Silicon-Substituted Carbonate Hydroxyapatite: Synthesis, Mechanical Properties, and Solubility Evaluations. *The Scientific World Journal*, *January 2015*. https://doi.org/10.1155/2014/969876

Barralet, J. E., Best, S. M., & Bonfield, W. (2000). *Effect of sintering parameters on the density and microstructure of carbonate hydroxyapatite*. *1*, 719–724.

Desiati, R. D., Sugiarti, E., & Ramandhany, S. (2018). Analisa Ukuran Partikel Serbuk Komposit NiCrAl dengan Penambahan Reaktif Elemen untuk Aplikasi Lapisan Tahan Panas [Particle Size Analysis of NiCrAl Composite Powders with Reactive Elements Addition for Thermal Barrier Coating Applications]. *Metalurgi*, *33*(1), 27. https://doi.org/10.14203/metalurgi.v33i1.358

Ezekiel, I., Kasim, S. R., Ismail, Y. M. B., & Noor, A. F. M. (2018). Nanoemulsion synthesis of carbonated hydroxyapatite nanopowders: Effect of variant CO32−/PO43− molar ratios on phase, morphology, and bioactivity. *Ceramics International*, *44*(11), 13082–13089. https://doi.org/10.1016/j.ceramint.2018.04.128

Filippov, Y. Y., Klimashina, E. S., Ankudinov, A. B., & Putlayev, V. I. (2011). Carbonate substituted hydroxyapatite (CHA) powder consolidated at 450°C. *Journal of Physics: Conference Series*, *291*(1). https://doi.org/10.1088/1742-6596/291/1/012036

Germaini, M. M., Detsch, R., Grünewald, A., Magnaudeix, A., Lalloue, F., Boccaccini, A. R., & Champion, E. (2017). Osteoblast and osteoclast responses to A/B type carbonate-substituted hydroxyapatite ceramics for bone regeneration. *Biomedical Materials (Bristol)*, *12*(3). https://doi.org/10.1088/1748-605X/aa69c3

Gibson, I. R., & Bonfield, W. (2001). *Novel synthesis and characterization of an AB-type carbonate-substituted hydroxyapatite*. *April*. https://doi.org/10.1002/jbm.10044

Haryati, E., Dahlan, K., Togibasa, O., & Dahlan, K. (2019). Protein and Minerals Analyses of Mangrove Crab Shells (Scylla serrata) from Merauke as a Foundation on Bio-ceramic Components. *Journal of Physics: Conference*

Series, *1204*(1). https://doi.org/10.1088/1742-6596/1204/1/012031

Jayasree, R., Madhumathi, K., Rana, D., Ramalingam, M., Nankar, R. P., Doble, M., & Kumar, T. S. S. (2018). Development of Egg Shell Derived Carbonated Apatite Nanocarrier System for Drug Delivery. *Journal of Nanoscience and Nanotechnology*, *18*(4), 2318–2324. https://doi.org/10.1166/jnn.2018.14377

Kadarisman, & Nurhasanah, I. (2020). BERDASARKAN ADSORPSI ISOTERM GAS NITROGEN Kadarisman dan Iis Nurhasanah. *Berkala Fisika*, *23*(3), 78–82.

Landi, E, Celotti, G., Logroscino, G., & Tampieri, A. (2003). *Carbonated hydroxyapatite as bone substitute*. *23*, 2931–2937. https://doi.org/10.1016/S0955-2219(03)00304-2

Landi, Elena, Tampieri, A., Celotti, G., Vichi, L., & Sandri, M. (2004). Influence of synthesis and sintering parameters on the characteristics of carbonate apatite. *Biomaterials*, *25*(10), 1763–1770. https://doi.org/10.1016/j.biomaterials.2003.08.026

Melinia, L. A., Puspita, E., Naibaho, M., Ramlan, R., & Ginting, M. (2022). Analisa Pasir Besi Alam dari Sungai Musi Sumatera Selatan. *Jurnal Penelitian Sains*, *24*(3), 122. https://doi.org/10.56064/jps.v24i3.716

Pieters, I. Y., Van den Vreken, N. M. F., Declercq, H. A., Cornelissen, M. J., & Verbeeck, R. M. H. (2010). Carbonated apatites obtained by the hydrolysis of monetite: Influence of carbonate content on adhesion and proliferation of MC3T3-E1 osteoblastic cells. *Acta Biomaterialia*, *6*(4), 1561–1568. https://doi.org/10.1016/j.actbio.2009.11.002

Ratner, B. D., Hoffman, A. S., Schoen, F. J., & Lemons, J. E. (2013). Introduction - Biomaterials Science: An Evolving, Multidisciplinary Endeavor. In *Biomaterials Science: An Introduction to Materials: Third Edition* (Third Edit). Elsevier. https://doi.org/10.1016/B978-0-08-087780-8.00153-4

Ratri, A. B. C. (2021). Pemanfaatan Limbah Cangkang Kepiting Sebagai Bahan Penambah Pakan Ternak Berkalsium Tinggi Dalam Tinjauan Moderasi Beragama. *Jurnal Pengabdian Masyarakat*, *2*(1), 101–124.

Ruiz, M. G., Hernández, J., Baños, L., Montes, J. N., & García, M. E. R. (2009). Characterization of Calcium carbonate, calcium oxide, and calcium hydroxide as starting point to the improvement of lime for their use in construction. *Journal of Materials in Civil Engineering*, *21*(11), 694–698. https://doi.org/10.1061/(ASCE)0899-1561(2009)21:11(694)

Rujitanapanich, S., Kumpapan, P., & Wanjanoi, P. (2014). Synthesis of Hydroxyapatite from Oyster Shell via Precipitation. *Energy Procedia*, *56*, 112–117. https://doi.org/10.1016/j.egypro.2014.07.138

Safarzadeh, M., Ramesh, S., Tan, C. Y., Chandran, H., Ching, Y. C., Fauzi, A., Noor, M., Krishnasamy, S., & Teng, W. D. (2019). Sintering behaviour of carbonated hydroxyapatite prepared at different carbonate and phosphate. *Boletín de La Sociedad Española de Cerámica y Vidrio*, 1–8. https://doi.org/10.1016/j.bsecv.2019.08.001

Surbakti, A., Oley, M. C., & Prasetyo, E. (2017). Perbandingan antara penggunaan karbonat apatit dan hidroksi apatit pada proses penutupan defek kalvaria dengan menggunakan plasma kaya trombosit. *Jurnal Biomedik (JBM)*, *Volume 9,* 107–114.

Wati, R., & Yusuf, Y. (2019). *Effect of Sintering Temperature on Carbonated Hydroxyapatite Derived from Common Cockle Shells (Cerastodermaedule): Composition and Crystal Characteristics*. *818*, 37–43. https://doi.org/10.4028/www.scientific.net/KEM.818.37

Wong, W. Y., & Noor, A.-F. M. (2016). Synthesis and Sintering-wet Carbonation of Nano-sized Carbonated Hydroxyapatite. *Procedia Chemistry*, *19*, 98–105. https://doi.org/10.1016/j.proche.2016.03.121

Yusuf, Y., Almukarrama, Permatasari, H. A., Januariyasa, I. K., Muarif, M. F., Anggraini, R. M., & Wati, R. (2021). *Karbonat Hidroksiapatit dari Bahan Alam: Pengertian, Karakterisasi, dan Aplikasi* (Moulidvi (ed.); Issue Oktober). Gadjah Mada University Press.